

Equilibrium Swelling of Polystyrene Networks by Linear Polystyrene

Thomas Russ,^{†,§} Rüdiger Brenn,[†] and Mark Geoghegan^{*,‡}

Fakultät für Physik, Universität Freiburg, Hermann-Herder-Strasse 3, D-79104 Freiburg, Germany,
and Department of Physics and Astronomy, Hicks Building, University of Sheffield, Hounsfield Road,
Sheffield S3 7RH, U.K.

Received July 24, 2002

ABSTRACT: We have measured the equilibrium swelling of polystyrene networks by linear deuterated polystyrene using the ion beam technique of helium-3 nuclear reaction analysis. These measurements enable an analysis of the swelling of networks at low degrees of swelling, and our results showed more swelling than predicted by using the usual forms of Flory–Rehner theory. The swelling of the networks by linear polymers can be explained if we consider the network as connected heterogeneous clusters which unfold during the swelling process. Reasonable results can also be obtained in terms of the Flory–Rehner model if a value of the Flory–Huggins interaction parameter is used that is dependent on the density of cross-links in the network. However, the resultant interaction parameter is negative, in contrast with the general result for isotopic mixtures. We were also able to swell the networks with linear polystyrene, which was initially mixed with high molecular weight polystyrene (which could not penetrate the network), and so were able to adjust the osmotic pressure of the swollen network. These results again cannot be analyzed by the usual Flory–Rehner theory, except when using a cross-linking density-dependent interaction parameter.

Introduction

The importance and ubiquity of polymer networks in many industrial processes lies in contrast to our present understanding of the basic physics controlling their behavior. Networks have many useful properties; their ability to dissipate energy over a large volume, for example, means that they can play an important role in adhesion. Another useful property, and one relevant to the present work, is the ability of a network to withstand exposure to solvents.

The swelling of polymeric networks by organic solvents has been the subject of research for some 60 years, with many theories and modifications to existing theories being proposed to explain swelling behavior. The debate about which theory is best is still largely a competition between that due to Flory and Wall^{1–5} and that due to James and Guth.^{6–9} We discuss these two theories below, but for now it is important to note that they have one property in common. In each case, the swelling of the network can be predicted from the free energy using a Flory–Huggins type lattice model. Indeed, we can write down one equation to describe both models, and this is generally known as Flory–Rehner theory.¹⁰ Whether we choose the Flory–Wall theory, or that due to James and Guth, depends simply on the values we give certain parameters. In this equation, the (Gibbs) free energy consists of two additive components, one due to mixing and one due to swelling. This additive property of the mixing and swelling terms precludes any possibility that the two may be somehow dependent on each other.¹¹ Indeed, this form for the free energy of a swollen network was criticized several years ago with the seminal differential swelling measurements of poly-

(dimethylsiloxane) networks by Neuburger and Eichinger.¹² They were able to vary the osmotic pressure of the networks by varying the solvent vapor pressure and found that neither the theory due to Flory and Wall nor that due to James and Guth could explain their results. Further work by Zhao and Eichinger¹³ sought to find a suitable theory to explain the swelling behavior of polymer networks, but a completely satisfactory theory proved elusive.

Despite the fact that the Flory–Wall equation failed to account for the results of Neuburger and Eichinger,¹² its use is still prevalent. Not only that, but the debate as to which of the two theories (Flory–Wall or James–Guth) is better at explaining the swelling behavior of polymer networks still continues to this day. The differences between the two theories are simple.^{1,14} In the Flory–Wall approach, the movement of the cross-links is restricted, whereas the junctions can travel through each other according to the theory due to James and Guth. For this reason, the James and Guth theory is usually called the “phantom model”, a terminology that we shall use. Although junctions cannot physically travel through each other, the phantom model is probably the more successful of the two at describing swelling because this model does allow the junctions greater freedom than the more affine model due to Flory and Wall. We shall therefore refer to the Flory–Wall approach as the affine Flory model.

There are various reasons for the continuing use of the Flory–Rehner theory. First, it is not unsuccessful. One can use it, for example, to describe the swelling of networks by small molecule solvents. Indeed, it is very often used to provide an estimation of the actual degree of cross-linking in the network from the total swelling. There are also other more subtle reasons as to why the Flory–Rehner theory has been successful. One is that it is simple and predictive. Given the theory and a few known parameters, we can predict the degree of swelling of a particular network. Not all theories are predictive, and Flory–Rehner will only be confined to history when

* Corresponding author. E-mail: mark.geoghegan@sheffield.ac.uk.

[†] Universität Freiburg.

[‡] University of Sheffield.

[§] Present address: IFM Electronic, Bechlinger Strasse 34, D-88068 Tettang, Germany.

a replacement comes along with equally suitable predictive properties, as well as better accuracy. The second more subtle reason for the success of Flory–Rehner theory is that it is instructive. This theory enables us to understand the basic principles of the swelling of polymer networks, i.e., the competition between entropy, elasticity, and enthalpy. This is in contrast to computer simulations, which will account for such behavior but not necessarily make the physics clearer to the interested scientist.

Although experiments such as those performed by Neuburger and Eichinger have not been successfully analyzed with the Flory–Rehner theory, this does not mean that the theory is necessarily incorrect, merely that the particular molecular models which were used are inappropriate. A convincing experimental demonstration of the inadequacy of the Flory–Rehner theory requires the failure of the additivity of the various energy terms. The attractiveness of Flory–Rehner as a means of considering polymer networks has, however, led many workers to extend and adapt the theory in search of a better solution. Many of these have been discussed in a brief review of some experimental tests of these models.¹⁵ The common thread linking all of these methods is that they all involve mean-field theory. The plethora of models present prevents us from considering each one in turn. However, in this work, we tabulate our results for swelling measurements, so the interested reader can compare particular theories with these results. More recent extensions to the Flory–Rehner theory^{16–19} brought some means of rationalizing the discrepancies between the original model of Flory and Wall to that of James and Guth. Furthermore, along with these ideas came the introduction of the use of an enthalpic interaction (χ -) parameter, which varies depending on the density of cross-links present in the network. The extension to include a cross-linking density-dependent χ -parameter will be treated in this paper because of the large amount of literature devoted to its use.^{20–31} Even here, however, it is difficult to find any consensus on the χ -dependence of the free energy. The χ -parameter is not necessarily the major contribution to the difference in free energy from the simple Flory–Rehner theory,^{20,22} and some also include a dependence of χ on solvent concentration.

Another form of mean-field theory is the rigorous replica approach.³² Although this method brings a mathematical rigor to the mean-field approach (arguably at the expense of clarity in understanding such networks), it is not readily experimentally testable.

In the present work, we therefore take the view that it is important to analyze the swelling of polymer networks in the light of Flory–Rehner theory. This will help us to further understand the limitations of the theory and ensure that, when it is used, it is used correctly. With the best usage of Flory–Rehner theory in mind, we shall also consider its extension with a cross-linking-dependent interaction parameter. Nevertheless, our swelling results will also be applied, where possible, to a simple scaling model developed elsewhere,³³ which considers the anomalous swelling of the networks.

One of the important factors in discussing the swelling of polymer networks is the existence of heterogeneities in the networks. Flory–Rehner theory considers the network as having a characteristic strand length (average distance between cross-link points), which is

uniform over the entire sample. Many small-angle neutron scattering (SANS) experiments have shown that this is not the case, largely by perturbing the network somehow, by either stretching^{34–37} or by swelling.^{20,34,36,37} The so-called “butterfly patterns”, observed by neutron scattering measurements,^{34–37} are a case in point.

Perhaps the most promising approach to a fuller understanding of the swelling of polymer networks has been to consider the networks as self-similar fractal structures. Here there are also different approaches to this problem. In one case, the network is considered as loosely connected fractal clusters. On swelling, the clusters deinterpenetrate (or unfold). These clusters are characterized by an inner fractal dimension that is only weakly dependent on the degree of cross-linking.³⁸ This was criticized as being unlikely in later work that suggested that this deinterpenetration would not occur.³⁹ In other words, the effect of the swelling would be local. Both ideas were further supported with computer simulations. However, the model networks used in the latter situation were end-linked with a Gaussian distribution of strand lengths, and it was accepted that in more heterogeneous systems (i.e., with many clusters or other defects such as “dangling ends”), the swelling argument would be pushed in the direction of the model due to Sommer and co-workers.³⁸ Both models can be approximated to scaling theories. In the model due to Sommer and co-workers, the size of the cluster is the relevant parameter, and it scales on swelling with a slightly larger exponent than the Flory exponent for the length of a polymer in a good solvent. The later (more local) model treats the network strands as the relevant length scale (as do the classical network elasticity theories), and here the scaling exponent, which is applied to the network strands, is somewhat larger than the Flory exponent (0.72 instead of 0.6). We shall not consider the latter model any further and point out that the scaling theory due to Sommer and co-workers has been extended and successfully applied to the data discussed in the present work.³³ We shall present the basic results, but the interested reader is referred to the original papers for the full details.

This work is part of a series of studies involved in elucidating many physical phenomena that occur with thin films of polystyrene networks. In each case, we have observed either direct or indirect evidence for heterogeneities. The first study considered the interface between a network and high molecular weight linear polymer.⁴⁰ In this situation, the high molecular weight linear polymer was not able to swell the network but could only penetrate it up to a certain distance. In several cases, the amount of penetration was observed to decrease with time, after an initial increase. This pointed to the existence of large-scale heterogeneities, which have their own, rather long, relaxation times. The same effect was noted in a later paper on the segregation of linear polymers from the network to a vacuum surface.⁴¹ In this case, the adsorbed amount was occasionally observed to decrease with time, again after an initial increase. In an investigation of the interpenetration of grafted polystyrene brushes into polystyrene networks,⁴² we observed that at, or close to, equilibrium, the amount of penetration of the network by the brush layer was independent of the cross-link density, at least over the range of cross-link densities studied. It is possible that the brush searched out regions of the

network with few cross-links, and if these regions were large enough, the average cross-link density would not be a major parameter. Finally and most directly, in measurements of the interdiffusion of a film of linear polystyrene into polystyrene network films,⁴³ we observed interdiffusion that appeared to be time dependent in some cases, pointing to the large-scale relaxation of heterogeneities. As well as this, we observed the interpenetration of the linear polymer layer by the network. We concluded that part of the network was being squeezed into the linear polymer during swelling. This is particularly interesting because it enables us to put a length scale on these heterogeneities, and they are particularly large, of the order of 100 nm or more.

In the present work, we describe experiments whereby we have swollen polystyrene networks with linear deuterated polystyrene (dPS). By working with thin films, we are able to achieve swelling equilibrium on experimentally accessible time scales. The swelling of a polymer network in its own melt is perhaps the ideal way of understanding the swelling of polymer networks for three reasons: First, the solvent is neutral. The linear polystyrene that we used is deuterium labeled, but this enthalpic interaction is very small and can often be neglected. Second, the degree of swelling can be altered by not only changing the cross-link density, but also by changing the length of the linear polymer. This is particularly useful because Flory–Rehner theory suggests that the ratio of these two parameters should be a universal scaling parameter that can describe the swelling. Finally, the success of Flory–Rehner theory is based upon swelling by small solvents. Any heterogeneities originally present in such systems have been essentially removed because of the high swelling ratio. As we have argued that heterogeneities are present over mesoscopic length scales in our model networks, it is worth investigating them. By swelling with linear polymers, we can only access small degrees of swelling. This means that the heterogeneities must still be present, and their effect should be observable.

This paper is divided up as follows: In the Experimental Section, we discuss the network preparation and characterization process as well as the helium-3 nuclear reaction analysis technique. We then discuss the Flory–Rehner theory by reviewing the affine Flory and phantom theories. Then we discuss the swelling equilibrium results and compare them to the predictions of these theories. We explain the deviations from these models by excluded volume effects, considering the network as a fractal structure. Before leaving the network swelling measurements, we present an analysis based upon the Flory–Rehner theory but with a cross-link-dependent interaction parameter. Finally we present measurements on a more general system where we are able to characterize the osmotic pressure and the free energy of the swollen polystyrene network during different swelling stages (and also to provide a comparison with the earlier experiments¹²). These data are again analyzed in the framework of the Flory–Rehner theory with a cross-linking density-dependent interaction parameter.

Experimental Section

Network and Sample Preparation. As the time scales that determine the movement of polymer chains in molten networks are so large, equilibrium structures can only be attained by the use of thin films. The model networks we use are either chemically prepared to obtain small mesh sizes

($N < 320$ in this study) or have been cross-linked by hydrogen ion irradiation resulting in larger mesh sizes ($N > 260$). We used a bilayer sample geometry with a linear polymer film placed on top of the network layer. The bilayer itself was supported on a silicon substrate. The linear polymer layer was spin coated onto a glass microslide before being floated off onto distilled water. It was then picked up onto the lower layer on silicon. The thicknesses of the network and initial melt layers (between 500 and 1000 nm) had to be tuned very carefully with respect to the amount of linear polymer that was left on the network surface after the network has been swollen to equilibrium. This layer had to be thick enough to provide enough polymer to completely swell the network and to be stable on the network surface without undergoing dewetting. However, the melt layer should not have been too thick such that the network layer was located so deep as not to be measurable. In the following, we describe preparation and characterization of the two network types.

Chemically Cross-Linked Networks. The synthesis has been described previously,^{35–37,40–44} but a more detailed version in the general literature is lacking and so is provided here. The reaction is a three-stage process; we use a Friedel–Crafts reaction and an exchange reaction to randomly functionalize the polystyrene with an aminomethyl group (NH_2CH_2), and the third stage is the cross-linking reaction.

First, monodisperse polystyrene dissolved in distilled dichloromethane (~4% w/v) was reacted under argon with *N*-chloromethylphthalimide (between 0.5 and 1% w/v) and SnCl_4 (~2 vol %) as catalyst to obtain the statistical copolymer poly(*p*-*N*-methylphthalimide styrene-*co*-styrene). The reaction to the ortho position on the aromatic ring is sterically hindered. The reaction continued for between 1 and 4 h before being stopped with a drop of tetrahydrofuran (THF). This reaction yields HCl and so it is important to wash the product until a pH value of 7 is achieved. The amount of *N*-chloromethylphthalimide and the reaction time are the parameters by which one can control the final amount of cross-linking. The modified polystyrene is then dried before being dissolved in THF (~5% w/v) and reacted under reflux with hydrazine, which was added to the solution dissolved to 5 vol % in ethanol. The resultant mixture contained 4 mL of THF to every 1 mL of ethanol. This reaction lasted typically 10 h. The resulting statistical copolymer is poly(*p*-aminomethylstyrene-*co*-styrene), sometimes called poly(vinylbenzylamine-*co*-styrene); the second reaction product is 2,3-dihydrophthalazine-1,4-dione. The two reaction stages are shown in Figure 1a. We characterize the amount of aminomethyl groups by acid–base titration or NMR. A typical acid–dose titration measurement would involve 100 mg of aminomethylated polystyrene dissolved in a mixture containing 27 mL of THF and 3 mL of water. Titration using infrared spectroscopy has shown these methods to be satisfactory.⁴⁴ To create a cross-linked network, the aminomethylated polystyrene is dissolved in toluene. To this solution we added the required amount of terephthalaldehyde (the cross-linker, also known as benzene-1,4-dicarboxaldehyde) dissolved in toluene. The resultant mixture was immediately spin cast onto a silicon wafer. In case a small amount of aminomethyl groups remain un-cross-linked, the reaction is brought to completion on further annealing for several hours in a vacuum oven at 185 °C. Figure 1b shows the cross-linking condensation reaction. As the process mainly takes place in a highly concentrated solution during spin casting, we can expect truly random cross-linking. Of course this process leads to densely and sparsely cross-linked regions, and these heterogeneities can have a profound effect on the network properties, as we shall describe in detail. Nevertheless, we believe these networks were created very close to the dry state and so are model random networks.

The bulky cross-link that we describe is slightly larger than two chain units and is not expected to be neutral to the linear polystyrene chains. However it should be dilute enough in order that enthalpic effects can be neglected. In contrast to networks created by, for example, a copolymerization process we do not expect aggregation of cross-links.^{45–48} By using high molecular weight precursor chains ($P > 2800$, where P is the

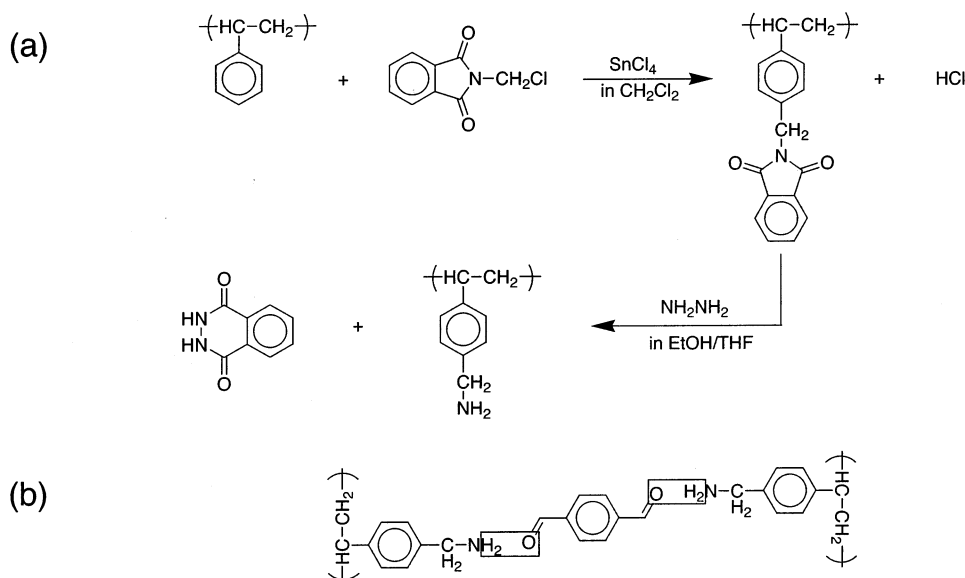


Figure 1. Chemical pathway to a statistical polystyrene network: (a) product after the first two stages, a statistical copolymer; (b) chemical reaction to form the cross-links in the networks during the spin casting process and during annealing.

polymerization index of the linear chains), we also reduce the amount of “dangling ends”. Therefore, the amount of sol in the networks is negligible and is washed out by toluene.

Irradiation-Prepared Networks. One disadvantage of the chemical preparation method for our model networks is that larger mesh sizes cannot be reliably prepared due to the presence of increasing sol. To avoid this problem, we achieved lower cross-link densities (large mesh sizes) by irradiating polystyrene films. The irradiation of polymers by UV or X-ray photons, ions, electrons, or α -particles modifies the material in several ways. The main processes are the formation of $\text{C}=\text{C}$ double bonds, chain scission, the creation of radicals, and, as a consequence, cross-links.⁴⁹ If the ion dose and the absorbed energy are kept low (~ 1 eV/atom), cross-linking is the dominant process in polystyrene and the stoichiometry of the system is preserved.⁵⁰

The network preparation was performed as follows: monodisperse polystyrene was dissolved in toluene and spin coated onto a silicon wafer, producing films of thicknesses of between 500 and 1000 nm. The polymer films were irradiated with 2 MeV H_2^+ ions (which break up into a pair of 1 MeV protons on impacting the sample surface) to create uniform networks of about 0.5×0.5 cm² size. Hydrogen ions were chosen because not too much energy is absorbed by the films as the ion decelerates (they have a low stopping power). This low stopping power of the hydrogen ions ensures that the ion energy and therefore the cross-link density remain relatively constant as a function of depth. To characterize the cross-link density of the irradiated samples we use the statistical theory of Inokuti.⁵¹ This theory takes into account the initial molecular weight distribution and the relation between the amount of chain scissions and cross-links. These parameters are well-known for polystyrene.⁵⁰ By knowing the gel fraction of an irradiated sample, we can calculate the mean number of cross-links per chain. We washed the irradiated samples with toluene to remove any sol created during irradiation. By measuring the thickness of the irradiated film by Rutherford backscattering (RBS) before and after washing in toluene, we were able to obtain the gel fraction. The gel fraction is given simply by the ratio of the film thickness in the washed sample to that before washing with toluene. By measuring the thickness of the washed sample at different points, we noted that the cross-link density was constant to within 10%.

To verify the statistical theory, we performed several tests: First, it is well-known that the number of cross-links increases linearly with ion dose.⁵² We confirmed this linear cross-linking dependence on the ion dose by using gel fractions with different precursor chain lengths. Second, there is a material specific

size that characterizes the amount of cross-links per unit energy absorbed in the sample. This size has been determined experimentally for polystyrene by several groups. The so-called G_x value (the number of cross-links for an incident dose of 100 eV) is obtained by measuring the gel point dose (the ion dose at which the gel point is reached): Hall et al.⁵³ obtained $G_x = 0.044$ cross-links for a 1.5 MeV H^+ beam, and Klaumünzer et al.⁴⁹ obtained $G_x = 0.051$ cross-links for a 0.3 MeV H^+ beam onto polystyrene. We calculated G_x by the statistical theory using the obtained gel fraction data and obtained $G_x = 0.040$ cross-links for our proton irradiation, which is consistent with the above results.

For characterization of the networks, we used a lower precursor molecular weight ($P = 327\text{--}1250$) to obtain low gel fractions, which enabled an exact determination of the relationship between ion dose and the number of cross-links. We used higher molecular weight polystyrene ($P = 3220$ and 6192) to create the networks used in the experiments, because this ensures negligible sol.

As a final step, having cross-linked the polymer, we washed the networks in toluene to remove any remaining sol. The starting molecular weight for the model networks is so high that we were not able to measure, within error, any sol. The error on the film thickness measurements by RBS is better than 10% but such a sol fraction would be inconsistent with our results for the low molecular weight characterization samples. We also annealed some networks for several hours to test the appearance of sol fraction during annealing due to sample degradation. No measurable degradation was observed.

Helium-3 Nuclear Reaction Analysis. To obtain the dPS concentration—depth profiles we used helium-3 nuclear reaction analysis.^{54,55} We here summarize the salient features. An incident beam of monoenergetic $^3\text{He}^+$ ions hits the sample and reacts with the deuterons to form ^5Li compound nuclei which quickly decay, creating protons and α -particles. The incident $^3\text{He}^+$ ions (and the emitted α -particles) are slowed by electronic collisions in the film. From the energy spectra of the emitted particles and knowing the differential cross section of the reaction, we can extract the volume fraction—depth profile of the deuterons and therefore the dPS.

For this work, we chose to detect protons because, although the resolution near the surface is slightly worse in comparison to α -particle detection,⁵⁶ at depth the resolution is somewhat better because protons lose almost no energy in exiting the sample. More importantly the count rate is much greater with proton detection (for the osmotic pressure measurements we sometimes used very low dPS concentrations).

The samples were placed at angles of between 15 and 30° to the beam and the detector at 165° to the beam. The resolution at the surface was between 30 and 80 nm depending on the angle between incident beam and sample and this resolution degraded slowly with increasing depth. The incident ion energy was 1.2 MeV.

Swelling Measurements

Theory. First we briefly review the Flory–Rehner theory of swelling. This theory has previously been used successfully to interpret many network swelling measurements using organic solvents^{57–59} and is based on the assumption that the total free energy of a swollen polymer network consists of the simple addition of elastic and mixing terms,

$$\Delta F = \Delta F_{\text{elastic}} + \Delta F_{\text{mix}} \quad (1)$$

It has often been proposed^{60,61} that the success of this theory might be due to the cancellation of two errors. The elastic energy is probably overestimated as excluded volume interactions are omitted in the simple Flory treatment and the mixing free energy is certainly also too large because correlations between cross-links and network chains are ignored.

The elastic energy term is analogous to that of a spring obeying Hooke's law and can be written as

$$\Delta F_{\text{elastic}} = \frac{N_g k_B T}{2N} (1 - \phi) (\lambda_x^2 + \lambda_y^2 + \lambda_z^2 - 3) \quad (2)$$

where N_g is the total number of lattice sites (we consider a lattice-type model, but N_g is equivalent to the total volume), N is the average number of monomer units between cross-links, k_B is Boltzmann's constant, T is the absolute temperature, and ϕ is the volume fraction of the solvent (linear chains) such that $1 - \phi$ represents the fractional volume occupied by the network. λ_i is the expansion in any one direction; if $\lambda_x = \lambda_y = \lambda_z = \lambda$, then expansion is isotropic and can be rewritten as $\lambda = (1 - \phi)^{-1/3}$. If, however, $\lambda_x = \lambda_y = \lambda_z = 1$, then there is no stretching and there is no elastic contribution to the free energy. In the case of swelling in one dimension, we have $\lambda_x = \lambda_y = 1$, and $\lambda_z = \lambda = 1/(1 - \phi)$. The prefactor Γ is a constant dependent on the nature of the network.

The mixing term can be given by

$$\Delta F_{\text{mix}} = N_g k_B T \left(\frac{\phi \ln \phi}{P} - \frac{\Phi}{2N} (1 - \phi) \ln(\lambda_x \lambda_y \lambda_z) + \chi \phi (1 - \phi) \right) \quad (3)$$

where P is the size of the solvent (linear polymer chain), Φ is another constant dependent upon the molecular model for the network that we choose, and χ is the Flory–Huggins enthalpic interaction parameter for the network and solvent. If the network is not prepared in the dry state, but rather at a volume fraction ϕ_s in a solvent, then $\lambda_x \lambda_y \lambda_z$ and $\lambda_x^2 + \lambda_y^2 + \lambda_z^2$ in the above two equations would need to be multiplied by ϕ_s and $\phi_s^{2/3}$ respectively. Here we consider $\ln(\lambda_x \lambda_y \lambda_z)$ to be a network entropy term. Although the network itself has a mass that should be considered infinite, the network strands can have entropy between two fixed junctions because they have a certain conformational freedom. If the junctions are not fixed in space, as in the phantom theory, then this term must disappear ($\Phi = 0$). The logarithmic term can also be considered to be part of

the elastic contribution to the free energy, in which case it is a term whose effect is to penalize compression.

In this paper, we shall consider both three and one-dimensional swelling. For the three-dimensional case, we obtain by adding eqs 2 and 3

$$\frac{\Delta F}{N_g k_B T} = \frac{3\Gamma}{2N} ((1 - \phi)^{1/3} - (1 - \phi)) + \frac{\Phi(1 - \phi)}{N} \ln(1 - \phi) + \frac{\phi \ln \phi}{P} + \chi \phi (1 - \phi) \quad (4)$$

For the affine Flory theory,^{1–5} $\Gamma = 1$ and $\Phi = 2/f$, and $\Gamma = (f - 2)/f$ and $\Phi = 0$ for the phantom theory.^{6–9} In our case the functionality is $f = 4$. Given that we are working with a simple bilayer system that is constrained to a substrate, the issue of dimensionality is important. Our samples show no evidence of swelling outside the limits imposed by the substrate. We have found in our previous experiments,^{41,43} however, that analysis using a one-dimensional swelling is not as successful as three-dimensional swelling. We have attributed the greater success of analysis assuming three-dimensional swelling to the presence of heterogeneities in the network, but nevertheless, we shall also test one-dimensional swelling. For one-dimensional swelling eq 4 becomes

$$\frac{\Delta F_{1D}}{N_g k_B T} = \frac{\Gamma}{2N} (1 - \phi) \left(\frac{1}{(1 - \phi)^2} - 1 \right) + \frac{\Phi(1 - \phi)}{N} \ln(1 - \phi) + \frac{\phi \ln \phi}{P} + \chi \phi (1 - \phi) \quad (5)$$

The equilibrium state is now defined by the equivalence of the chemical potentials inside and outside the network. We can set the chemical potential of the melt outside the network to zero and so obtain⁶²

$$\mu_a = \frac{1}{k_B T} \frac{\partial(\Delta F/N_g)}{\partial n_a} = \frac{-\phi_n^2}{k_B T} \frac{\partial(\Delta F/\phi_n)}{\partial \phi_n} = \frac{\Gamma(1 - \phi)^{1/3}}{N} - \frac{\Phi(1 - \phi)}{N} + \frac{(1 - \phi)}{P} + \frac{\ln \phi}{P} + \chi(1 - \phi)^2 = 0 \quad (6)$$

where n_a is the total number of linear chains and $\phi_n = 1 - \phi$. It is necessary to differentiate $\Delta F/N_g$ rather than ΔF because the number of lattice points increases as the network is swollen.

The affine Flory and phantom models are often considered as two limiting cases of the same theory. In the affine Flory model the junctions are embedded in the elastic continuum and are not able to fluctuate due to constraints imposed by other junctions. In the phantom model, the junctions can freely move and are not influenced by stretched chains. Experimentally, the swelling of a network by small molecule organic solvents can typically be better described by the phantom theory due to the increasing freedom of the junctions during the swelling process.¹⁴ It is important to note that these two models do not take into account excluded volume or other chain interactions due to entanglements. From eq 6, we obtain for the number of monomers between cross-links¹⁴

$$N = -\frac{P}{2} \left(\frac{(1 - \phi)^{1/3}(1 + G(\phi))}{(1 - \phi) + \ln \phi + P\chi(1 - \phi)^2} \right) \quad (7)$$

with $G(\phi) = 0$ for the phantom model and $G(\phi) = 1 - (1 - \phi)^{2/3}$ for the affine Flory model. The same is true of swelling in one dimension; by equating the chemical potential to zero in the one-dimensional case, we obtain

$$N = \frac{-P}{2(1 - \phi)} \left(\frac{1 + G_{ID}(\phi)}{\ln \phi + 1 - \phi + P\chi(1 - \phi)^2} \right) \quad (8)$$

where $G_{ID}(\phi) = 0$ for the phantom model, and $1 - (1 - \phi)^2$ for the affine Flory model. If ϕ_{eq} is the equilibrium fraction of dPS by volume in the network, we define

$$Q = 1/(1 - \phi_{eq}) \quad (9)$$

as the swelling ratio. Equations 7 and 8 are generalized in the sense that they can also be adapted to other developments of this theory, such as the constraint junction¹⁹ or slip-link models.⁶³ These particular models are not considered in the present work.

Because we are considering an almost athermal system, we note that P/N is a scaling parameter (if we assume $\chi = 0$) that does not depend on whether we use the affine Flory or phantom theory

$$Q = f_1\left(\frac{P}{N}\right) \quad (10)$$

where f_1 is a function chosen according to the model used.

In the above Flory–Rehner theory, the individual network strands provide the largest characteristic length scale. This means that the network is assumed to be homogeneously swollen. However there is experimental^{34,43} as well as theoretical evidence^{38,39} that statistical network structures display inhomogeneities on large scales. The so-called swelling anomaly at the onset of swelling,^{12,13,21,64,65} as well as some results from swollen or stretched networks, has not been explained by the classical theories above.^{34,35,37,43,66,67}

The classical models discussed above consider the individual network strand as the largest characteristic subunit, which determines the thermodynamic properties of the network. This assumption is based on a picture of a rather regularly ordered structure where heterogeneities have no influence on the proposed affine stretching behavior of the network chains. However, as explained in the Introduction, the relaxation behavior of statistical networks points to a very disordered inhomogeneous network structure, which is characterized by a rather nonaffine behavior. This is supported by the fact that the network strand lengths are exponentially distributed⁶⁸ and therefore extremely polydisperse, making affine behavior very unlikely. An alternative approach is to describe the swelling behavior of a statistical network in which the linear network chains are replaced by fractal objects.^{33,38} Their connectivity is characterized by a spectral (or internal) dimension $d_i > 1$. (The total number of monomers accessible by travelling n monomers along the topography of the network scales as n^{d_i} , defining the internal dimension d_i .³⁸ For linear chains $d_i = 1$.)

The network structure is considered to consist of strongly connected clusters of strands, which are only weakly connected to each other. For lower degrees of swelling, typically $Q < 2$, the swelling process can be illustrated with the picture of unfolding of larger clusters. Because the linear polymer is much smaller

than these clusters it acts as a good solvent. The movement of these large clusters is therefore driven by mutual excluded volume interactions. In other words, we are applying exactly the same principle governing the stretching of a single polymer chain in a good solvent. Individual clusters are connected either by long network chains, or by weakly connected substructures. The more cross-linked clusters are only weakly deformed, resulting in a nonaffine behavior of the whole network. However, if a good small molecule solvent were used to swell the network, even the more cross-linked clusters would unfold and deform. The total swelling would therefore represent an average behavior that can be characterized by the average length of a network strand. For this reason, linear polymers are very appropriate for rigorously investigating the swelling behavior of model polymer networks. Similarly, however, if the linear chains are too long, excluded volume interactions will vanish and an investigation of these large-scale structures will not be possible.

In using this model, Sommer et al.³³ were able to obtain a scaling parameter P^A/N , where A is dependent on the internal dimension of the clusters. Equation 10 is then modified to give

$$Q = f_2\left(z\frac{P^A}{N}\right) \quad (11)$$

where z is a fitting parameter.

Results and Discussion. In our experiments, we used networks with mesh sizes of between $N = 60$ and 2000 and polymerization indices of the linear polymers of $P = 138$, 313, 714, and 1696. The samples were annealed at 185 °C under vacuum. To verify that the swollen network was at equilibrium, we measured in each case a second identical sample that had been annealed for twice as long. If the dPS concentration remained constant we concluded that the samples had reached equilibrium. Typical annealing times necessary for attaining equilibrium were between 12 h for $P = 138$ and 1 week for $P = 1696$. The various values of N , P , and Q are listed in Table 1.

The use of two different network preparation methods gives our experiments a general character. First, we were able to cover a wide range of mesh sizes and second we could exclude preparation state effects on the equilibrium swelling as a dominant factor in our results (e.g., a swollen preparation state in the case of the chemical networks or a different structure due to chain scission in the case of ion beam cross-linked networks). We note that the swelling obtained for chemical ($N = 320$) networks is similar to the swelling obtained for comparable ion beam cross-linked networks (see Table 1) for all of the linear molecular weights considered. This was also the case for previous measurements of the interdiffusion of these linear polymers into these networks.⁴³ Although SANS measurements on poly(*N*-isopropylacrylamide) gels⁶⁹ showed that there are differences between γ -irradiated and chemically prepared networks, this must not be taken as a general result because, for the reasons pointed out above, we believe that both preparation methods used in the present work produce similar model random networks.

In Figure 2, we show data exemplifying the swelling. From these data we note that there is no depth-dependent swelling behavior (which would suggest depth-dependent cross-link densities). This is the case

Table 1. Relevant Parameters for the Networks Used in the Equilibrium Swelling Measurements, as Well as the Swelling Results for the Four Linear Polymers Used^a

mesh size, N	prep method	precursor polymn index	swelling ratio, Q			
			$P = 138$	$P = 312$	$P = 714$	$P = 1696$
60	chem	3221	1.22	1.18	1.03	1.01
110	chem	3221	1.47	1.25	1.09	1.02
120	chem	3000*		1.27		
320	chem	3221	1.67	1.43	1.25	
264	irr	3221		1.43		
308	irr	3221	1.89	1.52	1.28	
361	irr	3221	1.85	1.61	1.33	1.14
361	irr	6192				1.16
378	irr	3221				1.25
431	irr	6192				1.22
437	irr	3221	2.17	1.72	1.47	1.25
474	irr	6192	2.50	1.82	1.52	
534	irr	3221			1.54	1.39
559	irr	6192		1.85		
589	irr	6192			1.49	
610	irr	6192		2.00	1.67	
639	irr	6192	3.13	2.33	1.69	1.45
743	irr	6192		2.33		
763	irr	3221				1.43
853	irr	3221			1.82	
924	irr	6192		2.50	1.89	1.67
933	irr	6192				1.82
1066	irr	6192	4.00	2.94	2.11	
1388	irr	6192			2.08	
1933	irr	6192			2.86	
2078	irr	6192				2.50

^a The preparation methods referred to are the chemical method (chem) as well as irradiation prepared networks (irr). The precursor marked with an asterisk is polydisperse with a polydispersity of 2.

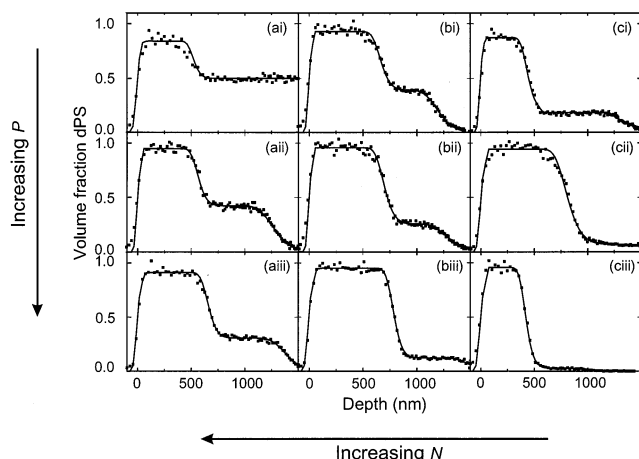


Figure 2. Sample ion beam equilibrium swelling data and fits. Spectra a–c are for mesh sizes of $N = 639$, 361 , and 110 , respectively. The latter network was created by the chemical method schematically illustrated in Figure 1 and the first two by ion beam irradiation. Spectra i–iii are for linear chains of $P = 313$, 714 and 1696 , respectively. The samples were annealed for between 3 days and 2 weeks at $185\text{ }^{\circ}\text{C}$.

for all of our data. The equilibrium dPS concentration at the surface of the network is nearly unity for all systems, with the slight discrepancy probably being due to the movement of heterogeneities within the system.⁴³ As expected, we observe a decrease in the swelling if we increase the molecular weight of the linear chains for a given value of the mesh size. We also note a decrease in Q for a given linear chain length with decreasing mesh size. As an example, in the case of $N = 60$ we observed no interdiffusion at all for chain lengths of $P = 714$ and 1696 but for $N = 110$ only $P =$

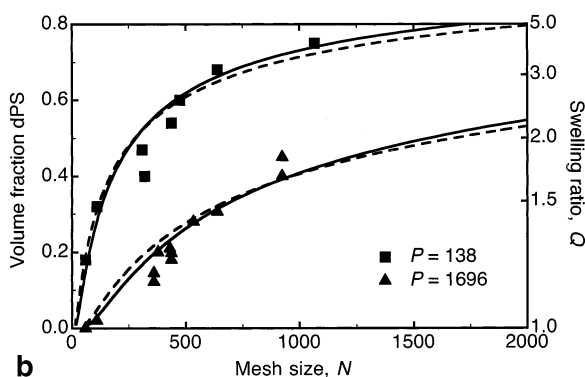
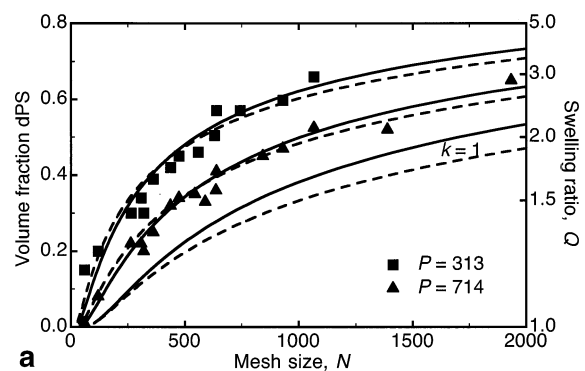


Figure 3. Experimental results for the equilibrium dPS volume fraction and the swelling ratios Q . The data are fitted using eqs 7 and 12. The dashed lines represent the affine Flory model; the solid lines, the phantom model. The relevant linear molecular weights are indicated in the figure. In part a, we also show the theoretical predictions for $k = 1$. The error in determining the mesh size is better than $\pm 10\%$. The uncertainty in the dPS volume fraction is less than $\pm 5\%$.

1696 did not swell the network. Previous experiments have shown diffusion into polystyrene networks to be completely inhibited when the linear polystyrene is of very high molecular weight.^{40,47}

In Figure 3, parts a and b, we show the experimentally obtained swelling ratios Q together with the predictions of the phantom and affine Flory model (eq 6). We observe swelling ratios Q larger than the calculated theoretical values for all mesh sizes and linear chain lengths. The results displayed in Figure 3 may be explained in terms of the Flory–Rehner theory if we assume that not every chain contributes to the network elasticity due to, for example, “dangling ends” or other finite branched structures, which might result in a smaller “elastic” osmotic pressure and a larger swelling ratio. To take into account elastically inactive chains we introduce an additional factor into eq 1 to weight the elastic energy

$$\Delta F = k\Delta F_{\text{elastic}} + \Delta F_{\text{mix}} \quad (12)$$

k is therefore used as a fitting parameter. In Figure 3, parts a and b, we also show the respective fits to the data using eqs 4 and 6 (modified using eq 12) for a varying mesh size with constant linear molecular weight. The values of k are shown in Figure 4 as a function of P . Both the affine Flory and phantom models give acceptable fits although for all molecular weights the phantom model works slightly better than the affine Flory theory (χ^2 is smaller). Within the scope of the classical models, the respective fit values of k must be considered as mean values averaged over all mesh sizes.

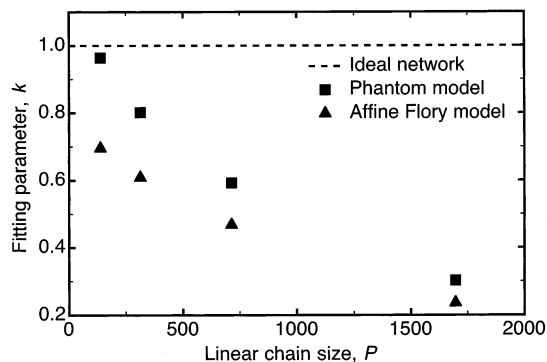


Figure 4. Fitting parameter k obtained for the different linear molecular weights (see eq 12). The fits corresponding to these values are shown by the solid and broken lines in Figure 3.

We could, for example, attach to every mesh size a different elastically effective number of network chains. We therefore could expect a slight increase of swelling if we increased the precursor molecular weight. To check this possibility we can compare measurements with different precursor molecular weights but similar mesh sizes. However, we did not observe any systematic change in swelling (see Table 1). This is also reflected by Figure 3, parts a and b, where the measurement values follow a continuous curve, although we used several precursor molecular weights.

As a next step, we compare the fitting parameters obtained for the different molecular weights (Figure 4). According to the Flory–Rehner theory, k should remain constant, as the elastic free energy should not depend on the different molecular weights of the solvent chains. The constancy of k results directly from the additivity of the free energy terms assumed in eq 1. In Figure 3, however, we see that there is a decrease of the contribution of the elastic free energy with increasing linear chain length. In the case of the lowest molecular weight ($P = 137$) we note that the fitting parameter tends to unity. This is consistent with conventional swelling measurements using good organic solvents where the Flory–Rehner theory works quite well.^{57–59} Although k not being constant suggests that the elastic and mixing energy terms cannot simply be added, it is equally possible that a different model (e.g., with a cross-link-dependent χ -parameter) may circumvent this failure of mean-field theory.

To summarize our data we present a master plot (Figure 5a), showing the swelling as a function of P/N (eq 10). According to the classical theories (eq 10), the measurement values should follow a single continuous curve, but the data display considerable scatter. Additionally we show the predictions of the affine Flory and phantom theories for perfect networks undergoing athermal swelling in one and three dimensions. We also show the prediction of the affine Flory model in three dimensions influenced by the small χ -parameter of the isotopic polystyrene blend (dPS/hPS)^{70–72} for a linear chain length of $P = 1696$. For the largest molecular weight, we obtain the largest shift from the athermal prediction. It is clear from Figure 5a that no repulsive enthalpic interactions are responsible for the observed behavior, as this would suggest the opposite behavior, e.g., less swelling for larger P/N . We also see from Figure 5a that the one-dimensional swelling models underestimate the measured swelling by a considerably greater amount than the predictions for three-dimensional swelling.

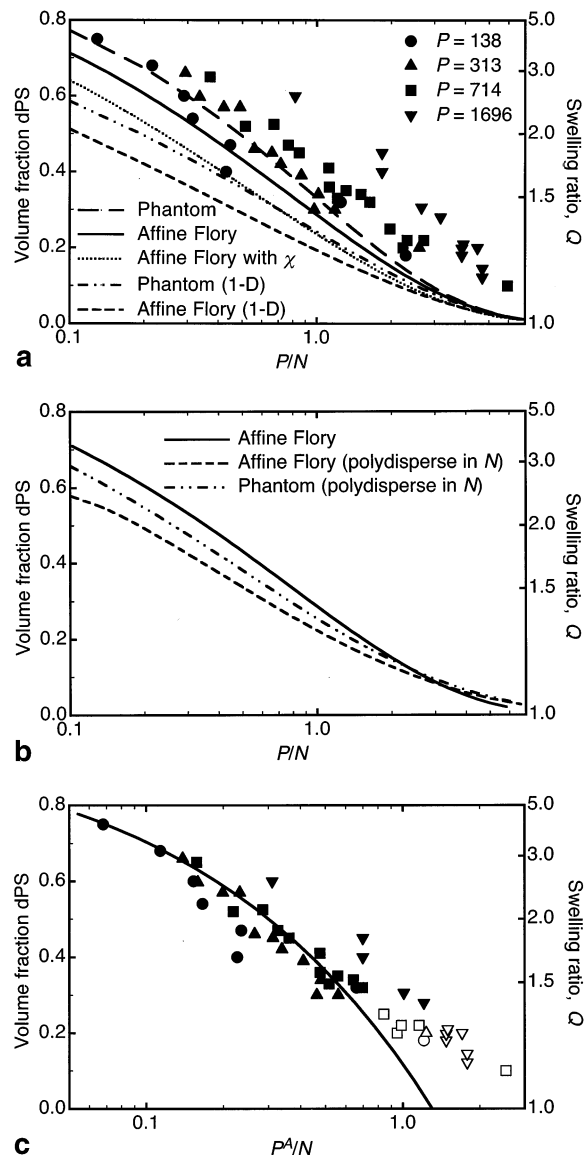


Figure 5. (a) Scaling plot for the different linear polymer molecular weights. The lines indicate the predictions of the affine Flory and phantom theories for both one and three-dimensional swelling, as well as the affine Flory theory for three-dimensional swelling including enthalpic effects for $P = 1696$. The data points do not collapse onto a single master curve as predicted by the affine Flory theory. (b) The prediction of the affine Flory theory (taken from part a), along with the predictions of the affine Flory and phantom theories for a polydisperse network with the cross-link density distribution given by $\rho_{\text{exp}} = (1/N) \exp(-N_i/N)$. (c) Master plot according to the recent scaling theory.³³ We used an internal fractal dimension $d_i = 1.10$ to obtain $A = 0.87$ (eq 11), using a fitting parameter dependent on the relative magnitudes of the mixing and elastic components in the chemical potential.³³ The curve is only fitted to points with a dPS volume fraction of greater than 0.25 (i.e., the open symbols were not considered in the fitting).

As our networks are statistical and not end-linked, we tried to take into account the mesh size distribution by a simple approximation within the classical theories. First we assumed that the network chain length distribution ρ is either Gaussian⁶⁸ or exponential.⁷³ (The correct treatment of network chain length is similar to that used to calculate mean free paths and transport coefficients in gases; the probability of a cross-link lying further than N_i monomer units from the previous cross-link is given by $(1/N) \int_{N_i}^{\infty} \exp(-N_i/N) dN_i = \exp(-N_i/N)$.)

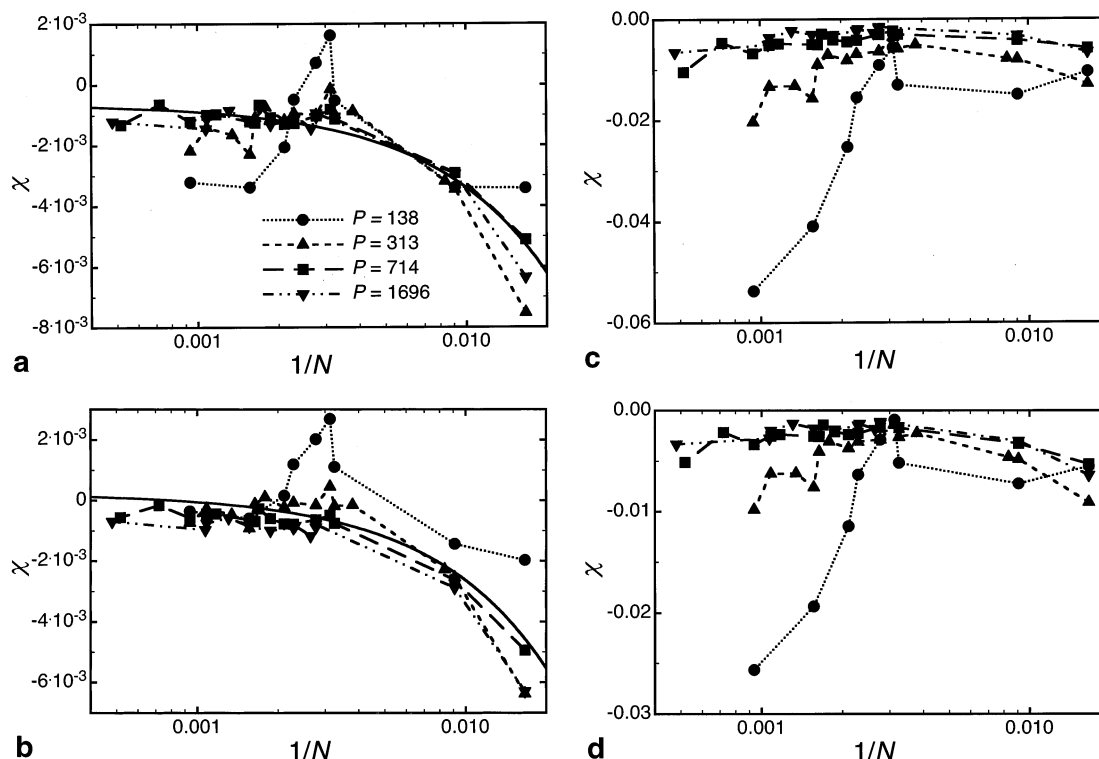


Figure 6. Interaction parameter plotted as a function of cross-linking density, $1/N$ for the four different linear chain sizes used in the present study. In part a, we show the interaction parameter as calculated using the affine Flory theory, and in part b, using the phantom model. The solid line is a fit to the data, given in part a by $\chi = 0.27712 - 0.277731 \exp(1/N)$ and in part b by $\chi = 0.285637 - 0.285419 \exp(1/N)$ (the lattice volume is based on a styrene monomer). Parts c and d show the same analysis as that for parts a and b, respectively, except that they indicate results for one-dimensional swelling. Because of the scatter in the results for χ using one-dimensional swelling, we do not fit to the data.

The network chain length distribution is thus expected to be exponential.) We then calculated the chemical potential of the network by adding the weighted contributions of the mesh sizes N_i and from eqs 7, 9, and 10, the equilibrium volume fraction is then given by (for $\chi = 0$)

$$\phi_{\text{eq}} = \sum_{N_i=1}^{\infty} \phi(N_i) \rho(N_i) \approx \int_1^{\infty} \rho(N_i) (1 - 1/f_1(P/N_i)) dN_i \quad (13)$$

with $\rho_{\text{exp}} = (1/N) \exp(-N/N)$ or $\rho_{\text{Gauss}} = (1/\sqrt{2\pi\sigma}) \exp(-(N - N)^2/2\sigma^2)$. The results of the Gaussian distribution for different values of σ yielded almost no change in the degree of swelling. This is in agreement with the theoretical results of Vilgis⁷³ for weakly inhomogeneous networks. In the case of the exponential distribution, a more noticeable deviation from the P/N -scaling behavior is observed. However, we observe a decrease of the quality of solvent (less swelling compared to the Flory–Rehner prediction for a single mesh size) with increasing linear chain length in contradiction to the results shown in Figure 5a. The decrease in swelling is simply because smaller mesh sizes are more likely than larger meshes. We show the predictions for the exponentially decaying cross-link density distribution in Figure 5b.

Cross-Linking Density-Dependent χ -Parameter.

As we mentioned in the Introduction, a school of thought has it that there is a cross-linking dependency to the χ -parameter. It is possible to fit our data to a floating χ -parameter in order to test this assumption. If the assumption that a cross-linking density-dependent χ -parameter could explain the swelling in our networks is

correct, the calculated value of χ should still be independent of linear polymer molecular weight. We show the results of such an analysis in Figure 6, parts a and b, and we see that this criterion is achieved. For all of the linear polymer molecular weights tested, the value of χ obtained from the swelling measurements is, within error, the same. In Figure 6, parts c and d, we also show the same analysis but for one-dimensional swelling. Although a much greater value (i.e., more negative) of χ can be used to fit the data, the same result for χ cannot be used for the different linear polymer molecular weights.

Previous work including a cross-linking density-dependent χ -parameter is not restricted to a particular molecular model for the elasticity of the network.^{22,25–30} A measured form of the elasticity can be included in the elastic term of the free energy. Under such circumstances, the Flory–Rehner hypothesis has shown to be able to explain the data. This is particularly useful for mechanical experiments, and does have the advantage of removing some experimental uncertainty. Such an approach in this work would mean that the debate over whether to use one or three-dimensional swelling is no longer being a problem because we should no longer be imposing a particular model on our analysis. However, direct measurements of the elasticity of our films would be difficult, and the replacement of a particular model by a system dependent measured parameter loses generality. Certainly, an understanding of the molecular model itself is necessary if we want to predict structure–property relationships for elastomeric materials.⁷⁴ In any case, our analysis provides perfectly acceptable agreement with the data without having measured the elasticity. Another situation noted in previous work is

where the value of χ was dependent on concentration, or degree of swelling (usually by a form similar to $\chi = \chi_0 + \chi_1\phi + \chi_2\phi^2$).^{17,24,30} We have imposed no such concentration dependence primarily because we do not need to, but also because we are considering low degrees of swelling, where any concentration variations are comparatively small in comparison to the case for small molecule solvents.

We also use the scaling model of Sommer et al.^{33,38} because we believe that heterogeneities play a dominant role in the swelling we measure. Sommer and co-workers obtained by computer simulation an internal dimension $d_i = 1.15$ for their networks.³⁸ As our networks are less cross-linked we consider this value to be an upper limit. If we use $d_i = 1.10$, we obtain for the exponent in eq 11, $A = 0.87$.³³ In Figure 5c, we present a new master plot where we have replaced the P/N scaling variable by $P^{0.87}/N$. It is clear that, by introduction of the exponent, the scaling behavior improves and the data start to collapse onto a single curve. Although the fitting is not perfect, in contrast to the classical theories discussed above, this new scaling theory does show the direction in which further refinements should be directed. In the scaling approach, the unfolding of the clusters can take place in a manner that accommodates sample geometry so the issue of dimensionality is not a great concern.

For higher degrees of swelling (or smaller linear chain lengths), our results begin to approach the predictions of the classical Flory–Rehner theory (Figure 4). This means that at higher degrees of swelling, the picture of individually stretched chains begins to be recovered. This is in line with many experiments showing that the Flory–Rehner theory is a good approximation for the description of equilibrium swelling of networks using organic low molecular weight solvents.

We have to emphasize that the above scaling theory is only applicable to our systems if we can assume the presence of much larger structures than, for example, a single network chain. With such an assumption, we believe that we can explain the swelling of polystyrene networks by linear polystyrene as being due to large-scale structures being driven apart by excluded volume interactions due to the presence of linear polystyrene acting as a good solvent for these structures.

Differential Chemical Potential of a Swollen Network and Its Melt

The experiments described in this section are motivated by measurements of the Eichinger group^{12,64} as well as those of Gee and co-workers,⁶⁵ who performed comparative vapor sorption studies on cross-linked and un-cross-linked polymer–organic solvent systems. These groups were able to measure the differential chemical potential $\Delta\mu$ of these two states for different degrees of swelling far below the respective equilibrium swelling ratio.

First, they noted that $\lambda\Delta\mu$ shows an anomalous peak with increasing squared swelling deformation λ^2 ($\lambda\Delta\mu$ was chosen because, according to phantom theory, it should be independent of λ^2). This peak cannot be explained using the phantom or affine Flory theories. Second, their results depended strongly on the solvent used. Using the simple version of Flory–Rehner theory, this solvent dependency is incompatible with the additivity of the elastic and mixing energy terms to calculate the total free energy of a swollen network (eq 1), as,

according to this assumption $\Delta\mu$ should depend only on the elastic free energy, which is independent of the particular solvent. Both Eichinger and Gee performed their experiments in a regime of low degrees of swelling, far away from equilibrium swelling by their solvents. For this reason such measurements were also accessible to the later theory of Sommer et al.³⁸

As mentioned above, the swelling of the networks by polymeric solvents takes place at similarly low deformation ratios. However, in contrast to the earlier experiments,^{12,64,65} the elasticity of the network chains is expected to play a much more dominant role and one would therefore expect to observe a different behavior of the differential chemical potential.

Simple Theory. We define $s = 1 - \phi_{\text{lin}}$, and $u = 1 - \phi_{\text{net}}$, where ϕ_{lin} and ϕ_{net} are the volume fractions of linear polymer inside a matrix of high molecular weight linear polymer and the volume fraction of linear polymer inside a polymer network matrix, respectively. We first consider the chemical potential of the linear polymer inside a network. This is given by⁶²

$$\mu_{\text{net}} = -u^2 \frac{\partial(F_{\text{net}}/u)}{\partial u} = -u^2 \frac{\partial}{\partial u} \left(\frac{3\Gamma}{2N} (u^{-2/3} - 1) + \frac{\Phi}{N} \ln u + \frac{1-u}{uP} + \chi(1-u) \right) \quad (14a)$$

which in turn gives

$$\mu_{\text{net}} = \frac{\Gamma}{N} (1 - \phi_{\text{net}})^{1/3} - \frac{\Phi}{N} (1 - \phi_{\text{net}}) + \frac{(1 - \phi_{\text{net}})}{P} + \frac{1}{P} \ln(\phi_{\text{net}}) + \chi(1 - \phi_{\text{net}})^2 \quad (14b)$$

For the linear polymer trapped inside a high molecular weight (P_{HMW}) matrix, we have

$$\mu_{\text{lin}} = -s^2 \frac{\partial(F_{\text{lin}}/s)}{\partial s} = -s^2 \frac{\partial}{\partial s} \left(\frac{1}{P_{\text{HMW}}} \ln s + \frac{1-s}{sP} \ln(1-s) + \chi(1-s) \right) \quad (15a)$$

yielding

$$\mu_{\text{lin}} = -\frac{(1 - \phi_{\text{lin}})}{P_{\text{HMW}}} + \frac{(1 - \phi_{\text{lin}})}{P} + \frac{1}{P} \ln \phi_{\text{lin}} + \chi(1 - \phi_{\text{lin}})^2 \quad (15b)$$

Equilibrium will be achieved when the two chemical potentials are equal. We write this as

$$\frac{\Gamma}{N} (1 - \phi_{\text{net}})^{1/3} - \frac{\Phi}{N} (1 - \phi_{\text{net}}) + \chi(1 - \phi_{\text{net}})^2 - \chi(1 - \phi_{\text{lin}})^2 = \frac{1}{P} \ln \frac{\phi_{\text{lin}}}{\phi_{\text{net}}} + \frac{(\phi_{\text{net}} - \phi_{\text{lin}})}{P} - \frac{(1 - \phi_{\text{lin}})}{P_{\text{HMW}}} \quad (16)$$

Samples and Data Analysis. We are able to measure the chemical potential of networks swollen by a polymeric solvent during different swelling stages by using two layers. The bottom layer is the polystyrene network, created either chemically or by proton irradiation, and the top layer consists of a mixture of high molecular weight polystyrene (HMWPS) ($P_{\text{HMW}} = 23\,100$) and a certain amount of deuterated lower molecular

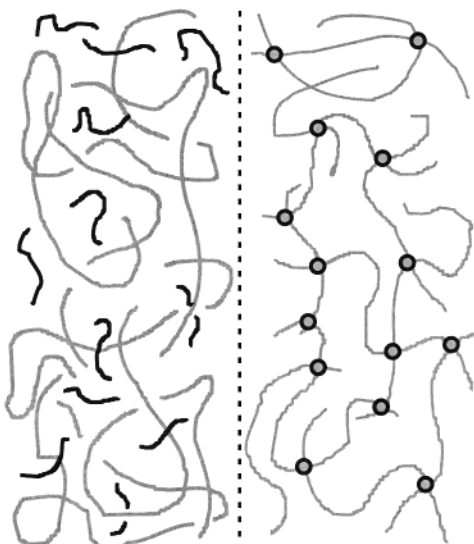


Figure 7. Schematic diagram of the sample geometry used to measure the differential chemical potential of a network and its melt. The right side of the broken line (interface) represents the network denoting the cross-links by circles, the left side the linear chain mixture. The black lines represent the shorter dPS chains, and the gray lines, the nondeuterated polystyrene (hPS) chains.

weight polystyrene (LMWPS) (Figure 7). We varied the total amount of LMWPS in the system to obtain different degrees of equilibrium swelling of the network after annealing. We ensured that there was no diffusion of the HMWPS into the networks by using large enough HMWPS chains.⁴⁰ As in the swelling experiments discussed above, we took care to check that the samples were in equilibrium after annealing. The total annealing time for all data in this section was 1 week at 185 °C.

We used networks of mesh sizes of $N = 308, 610$, and 320 . The latter network was created chemically, the former two by ion beam irradiation. For all linear molecular weights used (we use $P = 138, 313$ and 714), the square of the LMWPS chain length is similar to, or larger than, the HMWPS chain length. Following an argument discussed by de Gennes,⁶⁰ we conclude that, because $P^2 \geq P_{\text{HMW}}$, the un-cross-linked melt is ideal and free of fluctuations and that the HMWPS chains are not swollen by the LMWPS chains. Therefore, the state of the linear polymer mixture can be well described by mean-field theory. The linear polymer mixture then acts not only as a reservoir but also as a measure of the chemical potential of the network. We use simple Flory–Huggins theory to calculate the chemical potential of the linear polymer mixture, which is, at equilibrium, the same as that of the swollen network. Additionally, we use the dPS concentration in the network to calculate the chemical potential of the corresponding un-cross-linked melt. We therefore obtain for the differential chemical potential of the network–linear polymer system

$$\begin{aligned} \Delta\mu &= \mu_{\text{lin}} - \mu_{\text{net}} \\ &= \frac{1}{P} \ln\left(\frac{\phi_{\text{lin}}}{\phi_{\text{net}}}\right) + \frac{1}{P_{\text{HMW}}} \ln(1 - \phi_{\text{lin}}) + \frac{\phi_{\text{net}} - \phi_{\text{lin}}}{P} + \\ &\quad \chi((1 - \phi_{\text{lin}})^2 - (1 - \phi_{\text{net}})^2) \quad (17) \\ &\approx \frac{1}{P} \ln\left(\frac{\phi_{\text{lin}}}{\phi_{\text{net}}}\right) + \frac{\phi_{\text{net}} - \phi_{\text{lin}}}{P} \end{aligned}$$

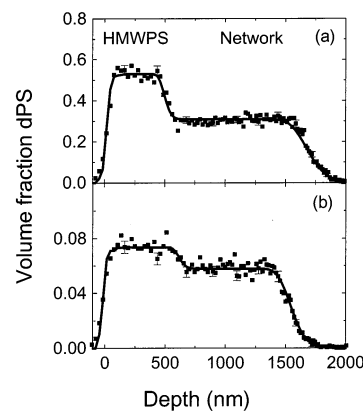


Figure 8. Two spectra obtained for the differential chemical potential measurements. The total amount of short dPS linear chains in the systems has been varied. In part a, the initial volume fraction of LMWPS is 0.67, and in part b, this value is 0.15. These two spectra have been obtained for the system with $N = 610$ and $P = 714$ by annealing at 185 °C for 1 week.

In the simplest Flory–Rehner treatment, we should neglect the entropic contribution of the HMWPS chains as well as enthalpic interactions due to the small χ -parameter.

In Figure 8, we show typical differential chemical potential data of an irradiation cross-linked network ($N = 610$) using $P = 714$. We analyzed the data by fitting a step function convolved with a Gaussian resolution function to the spectra to obtain ϕ_{lin} and ϕ_{net} .

Results and Discussion. First we note from Figure 8 that there is a larger concentration of smaller LMWPS chains in the linear matrix than expected from classical theory. As in the swelling experiments, we were able to confirm the validity of our results over a wide range of mesh sizes by measuring systems consisting of chemically and ion beam cross-linked networks. They all show the same behavior, which we discuss below.

In Figure 9a, we present results for the chemically cross-linked network with $N = 320$, in Figure 9, parts b and c, we show differential chemical potentials for the ion beam cross-linked samples with $N = 308$ and $N = 610$. With the exception of the $N = 610$ samples, we used all linear molecular weights mentioned above to measure the differential chemical potential. Each datum represents one spectrum. The abscissa represents the squared swelling deformation ratio $\lambda^2 = 1/(1 - \phi_{\text{net}})^{2/3}$. We note that $\lambda\Delta\mu$ decreases with decreasing elongation. The same behavior is also obtained for irradiation cross-linked networks with $N = 308$ and 610 using the same linear chain lengths. Within the figure we also show the predictions of the classical affine Flory and phantom models, which are given by

$$\Delta\mu^{\text{ph/aff}} = \Gamma \frac{(1 - \phi_{\text{net}})^{1/3}}{N} - \Phi \frac{(1 - \phi_{\text{net}})}{N} + \chi(1 - \phi_{\text{net}})^2 \quad (18)$$

For the curves without a χ dependence, we have simply set $\chi = 0$. The experimental data that are plotted in Figure 9 use the differential chemical potential given by

$$\Delta\mu = \frac{1}{P} \ln\left(\frac{\phi_{\text{lin}}}{\phi_{\text{net}}}\right) + \frac{\phi_{\text{net}} - \phi_{\text{lin}}}{P} + \chi_{\text{lin}}(1 - \phi_{\text{lin}})^2 \quad (19)$$

where χ_{lin} is the interaction parameter for the linear polymer blend. In principle, χ_{lin} should be the value of

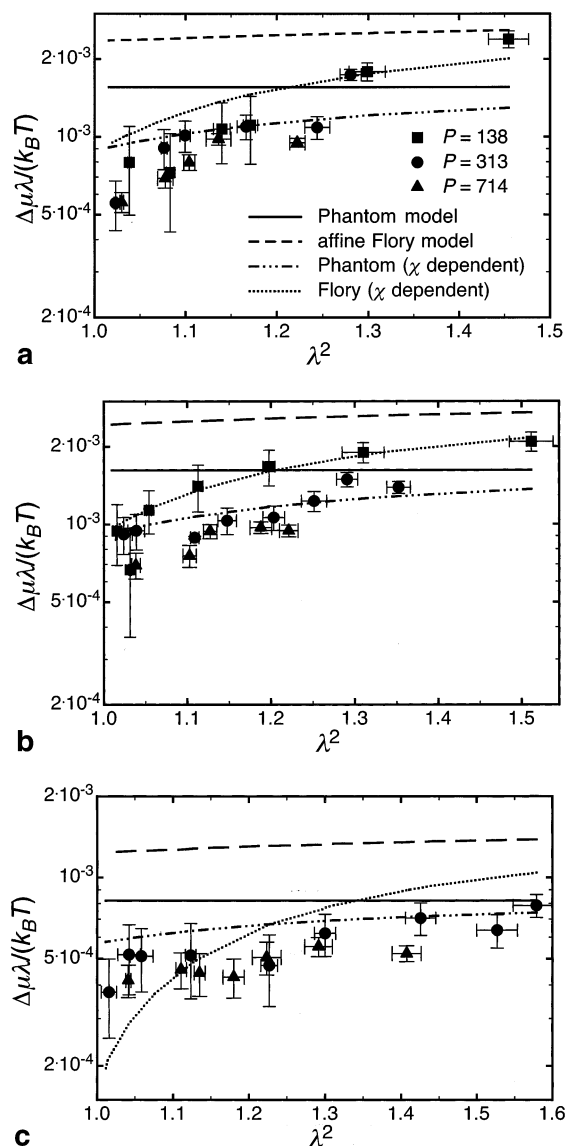


Figure 9. Differential chemical potentials multiplied by the swelling deformation ratio as a function of the squared swelling ratio. All linear molecular weights are shown together with the predictions of phantom and affine Flory theory. In part a, we show the results for the chemically created $N = 320$ networks; in parts b and c, the respective data for the ion beam cross-linked $N = 308$ and $N = 610$ networks are shown. In each case, we show the predictions of the phantom model and the affine Flory theory corrected for the χ dependence of the cross-link density calculated from the equilibrium swelling measurements. In all calculations, we neglected the contributions from the high molecular weight linear polystyrene.

χ measured for the networks extrapolated to zero cross-link density, but since χ_{lin} is a known experimental parameter measured to good agreement by several groups,^{70–72} it is sensible to use the known value. We use the value measured by Budkowski and co-workers⁷¹ of

$$\chi_{\text{lin}} = (1 - 0.18\phi_{\text{lin}}) \left(\frac{0.124}{T} - 0.000106 \right) \quad (20)$$

where we assume a lattice based on polystyrene monomer and T is the absolute temperature (here 458 K). A comparison between eqs 18 and 19 reveals consistency with eq 14, except for the omission of the entropic contribution due to the high molecular weight homopolymer, which has been neglected in this analysis.

Except, perhaps, for the $P = 138$ data of the $N = 308$ networks, all data for the various molecular weights follow single curves within the error bars. Neither the phantom theory, nor the affine Flory theory shows a similar strong decreasing trend of $\lambda \Delta\mu$. However, the use of the value of χ obtained from the swelling measurements improved the agreement considerably, with the phantom model probably giving the best fits overall.

We can also directly compare our results to the data obtained by Neuburger and Eichinger. Using low molecular weight solvents, they obtained a maximum for $\lambda \Delta\mu$ in the range of $\lambda^2 = 1.0$ – 1.1 .¹² None of our systems shows a similar maximum, even though we cover the same range. This disagreement probably reflects the elastic free energy playing a more dominant role swelling a network by a polymeric solvent than by a low molecular weight solvent (this does not however contradict the results shown in Figure 4 where the factor k , a measure of the number of elastically effective chains in the network, increases with decreasing P). For organic solvents, the elastic contribution can be considered as a small perturbation³⁸ providing ϕ is not too large. This is clear from eq 4 because, for organic solvents, $1/P \gg 1/N$. For polymer solvents, the mixing and elastic contributions become comparable as $1/N \approx 1/P$. It is also possible that there is some more subtle explanation for the peak in $\lambda \Delta\mu$ because it appears to be dependent on a variety of factors such as temperature and solvent.^{21,64}

In the present experiments, we are some way from equilibrium swelling. As a result of the low swelling, the unfolding of the clusters within the network is not yet realized, and the Gaussian elasticity assumed by Sommer et al.³³ cannot be applied. The swelling of these networks is governed by a virial expansion. The smaller the volume occupied by linear chains, the more important higher order terms become. Terms of higher order than the second-order term used by Sommer et al. are expected to lead to a different scaling exponent.

We therefore suggest a more qualitative explanation, which also supports the picture of the heterogeneous structure of a network. We propose that the expansion of the network at the beginning of swelling can be illustrated by the picture of the deinterpenetration of densely cross-linked clusters. At this stage of the swelling, the elastically effective chains are the interconnections of these clusters. If the solvent fraction is increased, the elastic free energy *not only* increases because of the increasing elongation of the chains but also increases because smaller network chains begin to contribute to the elasticity. We therefore have an increasing amount of elastically effective chains and a decrease in the mean mesh size N . In terms of eq 7, we may insert a volume fraction-dependent $N(\phi)$ which decreases monotonically with increasing elongation ratio (the value of z in eq 11 could be modified in the same way). The differential chemical potential is a direct measure of the additional elastic and entropic contributions of the network strands due to cross-linking. In Figure 9, we should therefore expect to see the effect of an increase in the amount of elastically effective chains as well as the solvent chains being forced to more densely cross-linked regions with increasing swelling. This qualitative model can also be compared with the picture of linear chains that are entropically trapped in “pores” of a heterogeneous medium.⁷⁵ Indeed, the idea

of entropic trapping being present in these networks is supported by the elongation of polystyrene brushes during the penetration of chemically prepared networks by polymer brushes.⁴²

On the Applicability of Mean-Field Theory

In this, and our earlier work,³³ we have presented two different forms of analyses for the swelling of polymer networks. We find that we can explain the swelling of polymer networks by treating them as a fractal system,³⁸ and analyzing the data using a simple scaling theory.³³ We can also achieve the same goal by using a modified Flory–Rehner approach based on the inclusion of a cross-link-dependent χ -parameter. The approach using a cross-link-dependent χ -parameter works slightly better if the phantom model is used as a basis for the analysis. We can also analyze differential swelling data with the same theory (again, the phantom theory is slightly better). In this case, the scaling theory does not provide a suitable examination of these data. Given the success of these two different approaches we here consider why we do not consider this modified Flory–Rehner approach to be the best way forward in considering the problem of network swelling.

The first argument concerns the value of χ . To fit our data correctly, a negative, N -dependent, interaction parameter must be used. The value of χ is increasingly more negative with increasing cross-link density. From the usual viewpoint of Flory–Huggins lattice theory, it is difficult to see how extra cross-links could increase the miscibility of the polymer in the network, particularly given that our experiments concern two different forms of cross-links. Furthermore, it is perhaps surprising that the increasing negativity of χ is not linear with increasing cross-link density; if we consider χ as a purely enthalpic interaction then by doubling the number of cross-links, we double the interaction energy and thus χ should be affected in the same way. Measurements on natural rubber have, however, shown that χ can increase linearly with cross-link density.²⁶ Recent SANS measurements of the interaction parameter between linear and branched polystyrenes have shown that χ is *positive* and *increases* with increasing number of branches.⁷⁶

Another important argument against the use of the modified Flory–Rehner theory is that it concerns three-dimensional swelling. Our samples only show swelling normal to the substrate; we see no lateral swelling. However, when we use one-dimensional swelling in our analysis, we have seen that the agreement with the data is much poorer than with three-dimensional swelling. We have also shown in this work that a cross-linking density-dependent χ -parameter cannot be responsible for this discrepancy because it varies with respect to the length of the linear chain. We have in the past considered one-dimensional arguments⁴⁰ with these networks but further experiments revealed that one-dimensional swelling provided poor agreement with the data (surface segregation of linear polymers from a network),⁴¹ or was completely unusable, as was the case for measurements of the interdiffusion of linear polymers into networks.⁴³ In the surface segregation measurements,⁴¹ we observed that there is far too little segregation of linear polymer to the vacuum surface predicted if we use one-dimensional swelling arguments to describe the phenomenon.

The use of mean-field theory in general has been criticized earlier in the paper. The criticism works on

two levels, provided one accepts the existence of large-scale heterogeneities in polymer networks.^{34,66} Regions of different swelling will need to have different free energies attributed to them. When these energies are added together, the result must equal the total free energy of the entire system evaluated at the mean values of ϕ and $1/N$. However, because the Flory–Rehner model is not self-consistent, this will not be the case. We have shown in a basic treatment (Figure 5b) that the polydispersity in network strand lengths results in a decreased swelling, rather than the increased swelling that we observed relative to the simple mean-field models. Considering such a problem rigorously is not a trivial matter and eventually leads to the use of the replica trick to solve the mean-field problem.^{32,77,78} Of course, such a complex statistical mechanical treatment is not necessary for polymer blends, or concentrated polymer solutions, because entanglements are not localized in space. A second problem, given the existence of large-scale heterogeneities is the inability of mean-field theory to predict them. The length scales relevant in mean field theory do not extend beyond the size of the linear chains and the average mesh size of the polymer.

The inability of mean-field theory to predict large-scale heterogeneities has led to a scaling theory for the elastic contribution to the free energy being developed in a mean-field context.²² In this work, the existence of excluded volume interactions is recognized through the mixing term in the free energy, but these interactions yield only a corrective prefactor to the original phantom model. With this approach, the importance of the χ -parameter is minimized although it is not neglected. (Another scaling theory for the elastic contribution to the free energy has been proposed and used for a description of the deswelling of polymer gels.)⁴⁸ Another attempt to consider an extra length scale in the mean-field model introduced a length scale that bounded nonaffine behavior from affine behavior.⁷⁹ Here the authors considered the effect of stretching on the size of the tube, within which the network chains are confined. Although this method was capable of predicting plausible stress–strain relations for polymer networks, its ability at predicting the actual heterogeneities resulting from SANS measurements has not been tested.

The use of mean-field theory to consider polymer networks is prevalent largely because it is in many cases successful. There are a variety of reasons why there has been so much success for mean-field theory. The success of mean-field theory (scaling theory extensions^{22,48} notwithstanding) hangs upon the absence of large-scale heterogeneities in the network, or because such heterogeneities have not been perturbed or revealed in any way. Our experiments, on networks cross-linked at, or very close to, the dry state, and only exposed to small degrees of swelling are a particularly good test of the existence of heterogeneities. Experiments on networks prepared in the swollen state^{20,22,24,30,48} are much less applicable, because, when deswollen, the network is likely to be much more isotropic than those described in the present work. Experiments performed on highly swollen networks are also more likely to be suitable candidates for a mean-field analysis. In this case, excluded volume cannot play a role, as the network is completely unfolded. The length scale of the network is then defined only in terms of an average strand length,

and N and P become the defining parameters. The trend toward this situation can be seen in our experiments from Figure 4, as the value of P is decreased.

Summary and Conclusions

We have presented measurements of the swelling of statistically cross-linked polystyrene networks by linear DPS chains. We have shown that this almost athermal system is ideally suited for the investigation of the equilibrium properties of networks at low degrees of swelling. We were also able to measure the chemical potential difference of the cross-linked and un-cross-linked systems during different stages of swelling. The use of two different methods of cross-linking ensures that we are confident about the generality of our results because the degree of swelling is independent of the method of sample preparation.

The detailed discussion of the results of both systems using both the phantom model, as well as the affine Flory theory, shows clearly that neither theory is suitable for predicting the swelling process at low degrees of swelling correctly. Consideration of enthalpic interactions (i.e., using a small positive χ -parameter taken from previously published measurements of isotopic linear polystyrene blends) or network strand length polydispersity, within this model, is unable to explain our experimental swelling results. The extension of the Flory–Rehner approach to include a cross-link-dependent interaction parameter is considerably more successful. We have been able to determine a value of χ from the swelling measurements that is dependent on the average density on the cross-links in the network. This value of χ is independent of the value of P , the linear polymer chain length. The application of this same value of χ to the differential swelling measurements is also successful. This success does come at the price of having a negative interaction parameter, which is not expected for the polystyrene system. Another difficulty with the current approach is that we needed a three-dimensional molecular model to provide an acceptable analysis of thin-film samples that only swell in one dimension. The equivalent one-dimensional model fails to provide a value of χ that is independent of linear chain length, P .

However, our swelling measurements support the idea of a network as a fractal object and can be explained with the resulting scaling law.³³ We emphasize that this scaling law can only be tested using athermal polymeric solvents ($\chi = 0$). The heterogeneous structure is taken into account by considering the network to consist of strongly connected clusters of strands that are only weakly connected to each other. Such structures result in a swelling process, which can be understood from the measurements on the differential chemical potential. The amount of elastically active chains increases and the mean mesh size decreases with an increasing degree of swelling. This behavior is considered to be responsible for the decrease of the differential chemical potential with decreasing elongation ratios. We conclude that large structures are involved in the swelling process. The relevant structural length scale of the network cannot be considered to be the single network strand.

Acknowledgment. T.R. thanks the Graduiertenkolleg *Strukturbildung in makromolekularen Systemen* for financial support. The authors would like to thank

Jens-Uwe Sommer (ICSI, Mulhouse, France) for many stimulating discussions. Professor G. B. McKenna (Texas Tech University) suggested the analysis of our data using a χ -dependent interaction parameter.

References and Notes

- (1) Flory, P. J. *Proc. R. Soc. London A* **1976**, *351*, 351.
- (2) Wall, F. T. *J. Chem. Phys.* **1942**, *10*, 132.
- (3) Wall, F. T. *J. Chem. Phys.* **1942**, *10*, 485.
- (4) Wall, F. T. *J. Chem. Phys.* **1943**, *11*, 527.
- (5) Wall, F. T.; Flory, P. J. *J. Chem. Phys.* **1951**, *19*, 1435.
- (6) James, H. M.; Guth, E. *J. Chem. Phys.* **1943**, *11*, 455.
- (7) James, H. M.; Guth, E. *J. Chem. Phys.* **1947**, *15*, 669.
- (8) James, H. M.; Guth, E. *J. Polym. Sci.* **1949**, *4*, 153.
- (9) James, H. M.; Guth, E. *J. Chem. Phys.* **1953**, *21*, 1039.
- (10) Flory, P. J.; Rehner, J., Jr. *J. Chem. Phys.* **1944**, *12*, 412.
- (11) Edwards, S. F.; Vilgis, T. A. *Rep. Prog. Phys.* **1988**, *51*, 243.
- (12) Neuburger, N. A.; Eichinger, B. E. *Macromolecules* **1988**, *21*, 3060.
- (13) Zhao, Y.; Eichinger, B. E. *Macromolecules* **1992**, *25*, 6996.
- (14) Erman, B.; Mark, J. E. *Structures and properties of rubberlike networks*; Oxford University Press: Oxford, England, 1997.
- (15) Gottlieb, M.; Gaylord, R. J. *Polymer* **1983**, *24*, 1644.
- (16) Erman, B.; Flory, P. J. *J. Chem. Phys.* **1978**, *68*, 5363.
- (17) Erman, B.; Flory, P. J. *Macromolecules* **1982**, *15*, 806.
- (18) Erman, B.; Flory, P. J. *Macromolecules* **1982**, *15*, 800.
- (19) Flory, P. J. *J. Chem. Phys.* **1977**, *66*, 5720.
- (20) Geissler, E.; Horkay, F.; Hecht, A.-M. *Phys. Rev. Lett.* **1993**, *71*, 645.
- (21) McKenna, G. B.; Crissman, J. M. *J. Polym. Sci., Part B: Polym. Phys.* **1997**, *35*, 817.
- (22) Geissler, E.; Horkay, F.; Hecht, A. M.; Zrinyi, M. *J. Chem. Phys.* **1989**, *90*, 1924.
- (23) Horkay, F.; Hecht, A. M.; Geissler, E. *J. Chem. Phys.* **1989**, *91*, 2706.
- (24) Horkay, F.; McKenna, G. B.; Deschamps, P.; Geissler, E. *Macromolecules* **2000**, *33*, 5215.
- (25) McKenna, G. B.; Douglas, J. F.; Flynn, K. M.; Chen, Y. *Polymer* **1991**, *32*, 2128.
- (26) McKenna, G. B.; Flynn, K. M.; Chen, Y. *Polymer* **1990**, *31*, 1937.
- (27) McKenna, G. B.; Flynn, K. M.; Chen, Y. *Polym. Commun.* **1988**, *29*, 272.
- (28) McKenna, G. B.; Flynn, K. M.; Chen, Y. *Macromolecules* **1989**, *22*, 4507.
- (29) McKenna, G. B.; Hinkley, J. A. *Polymer* **1986**, *27*, 1368.
- (30) McKenna, G. B.; Horkay, F. *Polymer* **1994**, *35*, 5737.
- (31) Douglas, J. F.; McKenna, G. B. *Macromolecules* **1993**, *26*, 3282.
- (32) Panyukov, S.; Rabin, Y. *Phys. Rep.* **1996**, *269*, 1.
- (33) Sommer, J. U.; Russ, T.; Brenn, R.; Geoghegan, M. *Europhys. Lett.* **2002**, *57*, 32.
- (34) Mendes, E., Jr.; Lindner, P.; Buzier, M.; Boué, F.; Bastide, J. *Phys. Rev. Lett.* **1991**, *66*, 1595.
- (35) Ramzi, A.; Zielinski, F.; Bastide, J.; Boué, F. *Macromolecules* **1995**, *28*, 3570.
- (36) Zielinski, F. Doctoral thesis, Université Pierre et Marie Curie, Paris, France, 1991.
- (37) Zielinski, F.; Buzier, M.; Lartigue, C.; Bastide, J.; Boué, F. *Prog. Colloid Polym. Sci.* **1992**, *90*, 115.
- (38) Sommer, J.-U.; Vilgis, T. A.; Heinrich, G. *J. Chem. Phys.* **1994**, *100*, 9181.
- (39) Pütz, M.; Kremer, K.; Everaers, R. *Phys. Rev. Lett.* **2000**, *84*, 298.
- (40) Geoghegan, M.; Boué, F.; Bacri, G.; Menelle, A.; Bucknall, D. G. *Eur. Phys. J. B* **1998**, *3*, 83.
- (41) Geoghegan, M.; Boué, F.; Menelle, A.; Abel, F.; Russ, T.; Ermer, H.; Brenn, R.; Bucknall, D. G. *J. Phys.: Condens. Matter* **2000**, *12*, 5129.
- (42) Geoghegan, M.; Clarke, C. J.; Boué, F.; Menelle, A.; Russ, T.; Bucknall, D. G. *Macromolecules* **1999**, *32*, 5106.
- (43) Russ, T.; Brenn, R.; Abel, F.; Boué, F.; Geoghegan, M. *Eur. Phys. J. E* **2001**, *4*, 419.
- (44) Bacri, G. Doctoral thesis, Université de Paris XI, Orsay, France, 1999.
- (45) Antonietti, M.; Sillescu, H. *Macromolecules* **1985**, *18*, 1162.
- (46) Briber, R. M.; Bauer, B. J. *Macromolecules* **1991**, *24*, 1899.
- (47) Wu, W.; Wallace, W. E.; van Zanten, J. H.; Bauer, B. J.; Liu, D.; Wong, A. *Polymer* **1997**, *38*, 2583.
- (48) Bastide, J.; Candau, S.; Leibler, L. *Macromolecules* **1980**, *14*, 719.

- (49) Klaumünzer, S.; Zhu, Q. Q.; Schnabel, W.; Schumacher, G. *Nucl. Instrum. Methods B* **1996**, *116*, 154.
- (50) Calcagno, L.; Compagnini, G.; Foti, G. *Nucl. Instrum. Methods B* **1992**, *65*, 413.
- (51) Inokuti, M. *J. Chem. Phys.* **1963**, *38*, 2999.
- (52) Calcagno, L.; Foti, G. *Nucl. Instrum. Methods B* **1991**, *59–60*, 1153.
- (53) Hall, T. M.; Wagner, A.; Thompson, L. F. *J. Appl. Phys.* **1982**, *53*, 3997.
- (54) Composto, R. J.; Walters, R. M.; Genzer, J. *Mater. Sci. Eng.* **2002**, *R38*, 107.
- (55) Geoghegan, M. In *Polymer Surfaces and Interfaces III*; Richards, R. W., Peace, S. K., Eds.; Wiley: Chichester, England, 1999 pp 43–73.
- (56) Jones, R. A. L. In *Polymer Surfaces and Interfaces II*; Feast, W. J., Monro, H. S., Richards, R. W., Eds.; Wiley: Chichester, England, 1993 pp 71–100.
- (57) Adachi, K.; Nakamoto, T.; Kotaka, T. *Macromolecules* **1989**, *22*, 3106.
- (58) Chatterji, P. R. *Macromolecules* **1991**, *24*, 4214.
- (59) Poh, B. T.; Adachi, K.; Kotaka, T. *Macromolecules* **1987**, *20*, 2563.
- (60) de Gennes, P.-G. *Scaling Concepts in Polymer Physics*; Cornell University Press: Ithaca, NY, 1979.
- (61) Hild, G. *Polymer* **1997**, *38*, 3279.
- (62) Brochard, F. *J. Phys. (Paris)* **1981**, *42*, 505.
- (63) Ball, R. C.; Doi, M.; Edwards, S. F.; Warner, M. *Polymer* **1981**, *22*, 1010.
- (64) Zhao, Y.; Eichinger, B. E. *Macromolecules* **1992**, *25*, 6988.
- (65) Gee, G.; Herbert, J. B. M.; Roberts, R. C. *Polymer* **1965**, *6*, 541.
- (66) Bastide, J.; Leibler, L.; Prost, J. *Macromolecules* **1990**, *23*, 1821.
- (67) Ramzi, A.; Hakiki, A.; Bastide, J.; Boué, F. *Macromolecules* **1997**, *30*, 2963.
- (68) Sommer, J.-U. *J. Chem. Phys.* **1991**, *95*, 1316.
- (69) Norisuye, T.; Masui, N.; Kida, Y.; Ikuta, D.; Kokufuta, E.; Ito, S.; Panyukov, S.; Shibayama, M. *Polymer* **2002**, *43*, 5289.
- (70) Bates, F. S.; Wignall, G. D. *Macromolecules* **1986**, *19*, 932.
- (71) Budkowski, A.; Steiner, U.; Klein, J. *J. Chem. Phys.* **1992**, *97*, 5229.
- (72) Green, P. F.; Doyle, B. L. *Phys. Rev. Lett.* **1986**, *57*, 2407.
- (73) Vilgis, T. A. *Macromolecules* **1992**, *25*, 399.
- (74) Mark, J. E. *Adv. Polym. Sci.* **1982**, *44*, 1.
- (75) Slater, G. W.; Wu, S. Y. *Phys. Rev. Lett.* **1995**, *75*, 164.
- (76) Greenberg, C. C.; Foster, M. D.; Turner, C. M.; Corona-Galvan, S.; Cloutet, E.; Quirk, R. P.; Butler, P. D.; Hawker, C. J. *J. Polym. Sci., Part B: Polym. Phys.* **2001**, *39*, 2549.
- (77) Ball, R. C.; Edwards, S. F. *Polymer* **1979**, *20*, 1357.
- (78) Ball, R. C.; Edwards, S. F. *Macromolecules* **1980**, *13*, 748.
- (79) Rubinstein, M.; Panyukov, S. *Macromolecules* **1997**, *30*, 8036.

MA0211885